Phase-transition behavior of *n*-alkanes on nanostructured polytetrafluorethylene films: Brillouin spectroscopic and calorimetric investigations on pentacosane

J. K. Krüger, R. Jiménez,* K.-P. Bohn, and C. Fischer
Fachrichtung Experimentalphysik 10.2, Universität des Saarlandes, Bau 38, Postfach 151150, D-66041-Saarbrücken, Germany
(Received 6 March 1997)

Large monocrystalline domains of pentacosane ($C_{25}H_{52}$) have been prepared on nanostructured polytetrafluoroethylene films. The acoustic and thermal properties have been investigated around the various phase transitions of the crystalline state of pentacosane using high-performance Brillouin spectroscopy and modulated differential scanning calorimetry. In the crystalline orthorhombic phase the values of the elastic constants are $c_{22}=7$ GPa, $c_{33}=35$ GPa, $c_{44}=2$ GPa. In the R_V orthorhombic rotator phase the elastic constants are $c_{22}=3.35$ GPa, $c_{33}=3.67$ GPa, $c_{44}<0.05$ GPa. The evidenced thermal and acoustic anomalies are discussed in the frame of the accompanying structural changes. [S0163-1829(97)00737-6]

I. INTRODUCTION

The interesting phase-transition behavior of linear telomers, especially the rotator transitions in *n*-alkanes, cycloalkanes, and perfluoroalkanes, etc. are due to a complicated interaction of intramolecular and intermolecular instabilities.[1–5] Usually the structural transitions in these systems have an order-disorder as well as a displacive character. This is reflected by acoustic as well as by thermal properties.[6–9] The competitive influences of the stiff covalent bonded chain molecules and the weak intermolecular interactions between the molecular chains as well as between the crystal lamellas on the elastic properties have been demonstrated for different types of alkanes.[5–7,10,11] Consequently, investigations of the static and dynamic elastic properties, combined with investigations of the thermal properties, will give essential information about the interrelations between these properties on one hand, and the molecular structure, the molecular dynamics, and the morphology on the other.

Unfortunately, investigations of the elastic properties of alkanelike crystals are handicapped by the lack of suitable single crystals.[12] However, the lack of suitable sample material did not hinder studies in the field and led to interesting unconventional solutions of this difficult experimental task. Pioneering ultrasonic work was done by Pechhold[13] in polycrystalline paraffins, by Heyer, Buchenau, and Stamm[14] using the inelastic neutron-scattering method developed by Buchenau,[15] and by Strobl and co-workers[16,17] who determined elastic compliances of $C_{33}H_{68}$ by the use of LAM Raman modes. More recently Snyder *et al.*[18] performed an analysis of the longitudinal acoustic modes (LAM) modes and proposed a chain-length dependence of the interlamellar elastic constant c_i. All these methods are indirect ways to determine the elastic properties of *n*-alkanes. Brillouin spectroscopy (BS) yielded first directly measured elastic constants of thin monocrystalline films of solution grown $C_{36}H_{74}$.[10,11] Marx and co-workers[6,19,20] introduced a Brillouin technique which is able to evaluate the elastic stiffness properties of alkane single crystals investigating mesoscopic single-crystalline domains of the polycrystalline material.

Recently we have tested a method to prepare thin macroscopic, nearly defectless crystal plates of *n*-alkanes or perfluoroalkanes.[7,8] This crystal growth method uses the polytetrafluoroethylene (PTFE) induced alignment (PIA) technique, to obtain oriented crystal plates of *n*-alkanes or perfluoroalkanes. The PIA technique, originally developed by Wittmann and Smith,[21] allows one to obtain highly structured crystal mats of very different materials including *n*-alkanes and perfluoroalkanes.[7,8,22–26] Although the organization mechanism of the nanostructured PIA substrate on the deposited sample material is not well understood, it is clear that the PIA substrate induces a preferential orientation of the sample crystallites with their *c* axes parallel to the preferential orientation of the PTFE. Usually, even a second crystallographic axis is positioned within the PIA plane.[7,8]

The aim of the current paper is to show that the transcrystallization mechanism on the PIA substrate still works for $C_{25}H_{52}$ and that the created morphology corresponds to that of solution- or melt-grown crystals of that material. Moreover, we want to relate our Brillouin and calorimetric investigations to the phase transition sequence and the related phase-transition mechanisms. We base our investigations on the interesting structural studies of Broadhurst,[27] Doucet *et al.* ,[28] Ungar,[29] and Sirota and co-workers.[9,30] According to this literature, the room-temperature phase is orthorhombic with the space group $Pcam$,[9,28–30] and a bilayer stacking of the lamellas ($ABAB\ldots$). The crystallographic *c* axis is directed along the molecular chain axis and the ratio between the *a* and *b* axis is $a/b\approx 1.5$.

The phase sequence in the case of $C_{25}H_{52}$ is similar to that found in other odd paraffins. The crystalline orthorhombic phase transforms at $T_k\approx 320$ K into a first rotator phase denoted as the R_V phase, observed by Ungar[29] and characterized in detail by Sirota *et al.* using x-ray diffraction.[30] According to Sirota *et al.* the symmetry as well as the layer stacking are maintained in this phase, however the molecules are tilted with respect to the layer normal by an angle of $\theta \approx 10°$. On increasing the temperature, the molecular tilt continuously decreases, vanishing at $T_1\approx 321$ K, the transition temperature into the R_I rotator phase.

The R_I phase also has an orthorhombic symmetry [space group $Fmmm$ (Ref. 29)], the layers still ordered by a bilayer

stacking. As already mentioned above, in this phase, the molecules are oriented again parallel to the surface normal. The transition from the R_V into the R_I phase is of second order as evidenced by Sirota *et al.*[9] and confirmed by our own measurements (see below).

A rhombohedral R_{II} rotator phase is found above $T_2 \approx 322$ K [space group $R3m$ (Ref. 29)]. This phase shows a strong dynamical disorder of the molecules favoring the average hexagonal packing within the lamella. Furthermore the layer stacking changes from bilayer ($ABAB\ldots$) to trilayer ($ABCAB\ldots$).

As has been shown for many systems,[6–8,10,11] the elastic properties of plastic systems are strongly affected by the morphology and the morphological changes during the different phase transitions. In the following, we will demonstrate the efficiency of high-resolution BS in connection with modulated differential scanning calorimetry (MDSC) investigations for the understanding of the dynamical properties of the system under study throughout its different phase transitions.

II. EXPERIMENTAL

Sample preparation: The raw material of $C_{25}H_{52}$ was purchased from Applied Science Laboratories Inc. and had commercial purity grade. The PIA technique to prepare sandwich samples has been described in detail in previous papers.[7,8,22–25] Here we only want to stress the most important aspects relevant for the present work. The PIA substrate consists of a highly oriented and highly crystalline PTFE layer of about 10 nm thickness usually deposited on a conventional glass substrate.[21] For further discussion we introduce an orthogonal sample coordinate system: the two axis and the three axis are directed within the plane of the PIA substrate, having the three axis oriented along the preferential orientation of the PTFE, the one axis is orthogonal to the film plane. Two such glass-PIA plates are used to build a cell (PIA sandwich cell) having (i) the PIA substrate at the inner surfaces of the cell and having (ii) the preferential direction of the PTFE molecules on the glass slides aligned in the same direction. The spacer between the glass-PIA plates had a typical thickness of $d = 10\ \mu$m. For the filling procedure both the cell and the Pentacosane sample are heated to a temperature above the melt temperature $T_m = 327$ K of $C_{25}H_{52}$. Usually the cell is filled using the capillary effect. Subsequent rapid cooling of the sample to ambient temperature usually leads to the appearance of cracks perpendicular to the three axis of the sample cell. They are due to heteronucleation and/or to thermally induced stresses originating from the different thermal-expansion coefficients between the sample and the glass support. Unfortunately, these cracks act as very efficient diffraction gratings for the laser light used for the Brillouin experiments. In order to reduce the number of these defects significantly, we developed a modified Bridgman crystal-growth technique described elsewhere.[31] The crystallization was performed at a rate of $\Delta T/\Delta t = 0.005$ K/min. After this crystallization procedure, the sample plate can be floated away from the glass plates yielding a free standing crystalline sample. It should be stressed that the PIA substrates, nanosized in one dimension, remain on the top and the bottom of the sample plate, respectively. According to preliminary x-ray investigations the crystallographic c axis of $C_{25}H_{52}$ is directed along the three axis and the a axis is orthogonal to the sample plate,[32] i.e., along the one axis of the sample cell.

Modulated DSC: The sample used for these measurements was a conventional $C_{25}H_{52}$ not oriented with the PIA technique. The calorimetric investigations were performed with a commercial Thermal Analyst 2920 system from TA Instruments Inc. with modulated differential scanning calorimetry (MDSC). In order to provide an adequate stable temperature environment of the MDSC oven during experiments performed in the time domain, we built a special cooling assembly described elsewhere.[33] Then, the periodic modulation of the temperature allows the immediate determination of the specific-heat capacity c_p at a given temperature[34] with the desired accuracy. The sinusoidal modulation of the exciting temperature signal was set to an amplitude of 0.1 K, the corresponding frequency was chosen as 16.7 mHz. This modulation corresponds to an oscillating rate with an amplitude of 0.63 K/min. The absolute temperature accuracy is about ± 0.5 K.

In order to be able to study very slow kinetic (time-dependent) thermal effects at constant temperature we used time-domain-MDSC (TDMDSC):[33] in the first step the sample is heated to a desired average temperature $\langle T \rangle$, after the stabilization of this temperature, the instantaneous specific-heat capacity, $c_p^i(\langle T \rangle)$, is recorded, subsequently the c_p measurements are repeated until the relaxed value, $c_p^r(\langle T \rangle)$, is approached. The next temperature step to a new temperature $\langle T + \Delta T \rangle$ is started only after the evolution of $c_p^r(\langle T \rangle)$. We used $\Delta T = +0.1$ K close to phase transitions and $\Delta T = +0.2$ K otherwise. The accuracy of the transition temperatures deduced from the measured $c_p(T)$ curves strongly depends on the sharpness of the transition features within this curve. We estimate this accuracy to be about ± 0.5 K.

Brillouin spectroscopy: All Brillouin measurements were performed with a five-pass Brillouin spectrometer taking advantage of the 90A scattering geometry.[35–37] Using an argon-ion laser at a wavelength of $\lambda_0 = 514.5$ nm, the acoustic wavelength amounts to $\Lambda = 363.8$ nm and is essentially independent of the optical refraction properties of the sample.[37,38] For a given acoustic wave vector $q = \hat{q}(2\pi/\Lambda)$ ($\hat{\mathbf{q}}$ is a unit vector pointing along $\mathbf{q}$) and knowing the mass density ρ of the material, the corresponding elastic stiffness constants can be calculated by $c(\Phi) = \rho[f^{90A}(\Phi)\Lambda]^2$. ρ is the mass density, f^{90A} is the phonon frequency, and Λ is the phonon wavelength. Φ is defined as the polar angle of the phonon wave vector with respect to the three axis within the sample plane, i.e., for the (2,3) plane $|\hat{\mathbf{q}}| = (0, \sin\Phi, \cos\Phi)$ holds. The elastic properties of the room-temperature phase of $C_{25}H_{52}$ on the PIA substrate were characterized in detail in a previous paper.[31] As has been shown in that paper, the combination of different scattering techniques[35–37] allows rather easily the determination of the whole elastic tensor of an alkane single crystal.

It is worth noting that for phonon propagation along the three and two axes ($\Phi = 0°$ and $\Phi = 90°$, respectively) the related elements of the elastic stiffness tensor c_{22}, c_{33}, c_{44}, c_{55}, and c_{66} can, in principle, be determined directly.[39] Tak-

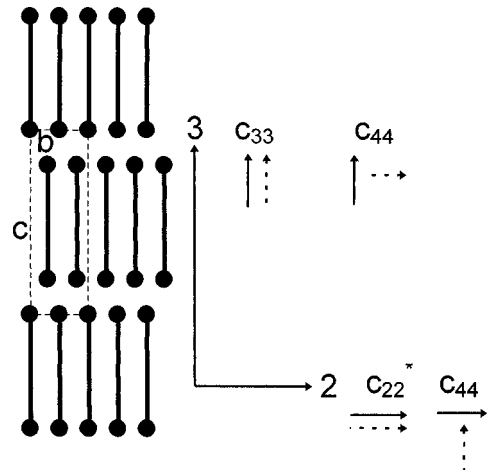

FIG. 1. Schematic representation of the relationship between the elastic constants and the crystallographic axes in the orthorhombic crystalline phase of $C_{25}H_{52}$. c_{22}^* corresponds to the pure longitudinal elastic constant c_{22} constant for phonon propagation along the crystallographic b axis only in the orthorhombic phases. In the rhombohedral R_{II} phase, c_{22}^* is the effective elastic constant for phonon propagation along the ''old'' crystallographic b axis. Full arrows: direction of phonon propagation, dashed arrows: direction of phonon polarization.

ing into account the orientation of the pentacosane crystals on the PIA substrate and the shortened Voigt's notation[39] of the elastic constants, it is straightforward to correlate the longitudinal polarized phonon mode propagating along the crystallographic c axis (three axis) with the elastic constant c_{33} and that propagating along the crystallographic b axis (two axis) with the elastic constant c_{22}. The elastic constants c_{44}, c_{55}, and c_{66} are the shear constants related to the sample plane (see Fig. 1).

However, the possibility for the determination of all these constants largely depends on the Pockels coefficients involved. Unfortunately, shear phonons often have a small scattering cross section. As a consequence, it is sometimes difficult to decide whether a shear phonon is missed because of its weak scattering cross section or because it is overdamped.[7,8,10,11] In the rotator phases of $C_{25}H_{52}$ both effects seem to accumulate. It should also be mentioned that Brillouin measurements on films of only 10 μm thickness are not at all an easy task. In order to properly evaluate the elastic constants of $C_{25}H_{52}$ as a function of temperature, we used the following densities: Until $T_1 = 320$ K, the density value $\rho = 951.9$ kg/m^3 was used.[28] Because of the lack of information about the precise temperature dependence of the density above T_1, we simply used the density value $\rho = 871.5$ kg/m^3.[28] We are aware of the fact that by maintaining the density at a constant value, we introduce a small inaccuracy in the determination of the elastic moduli. According to Doucet *et al.*[28] it decreases nearly continuously about 1% from T_1 until T_m but the data are spread too much in order to draw more precise conclusions. In any case, the presented values are proportional to v^2 ($c = \rho v^2$). Furthermore, this assumption seems to be justified since all experimental anomalies observed are more than one order of magnitude larger than any expected anomaly in the temperature dependence of the density ρ.[28,30]

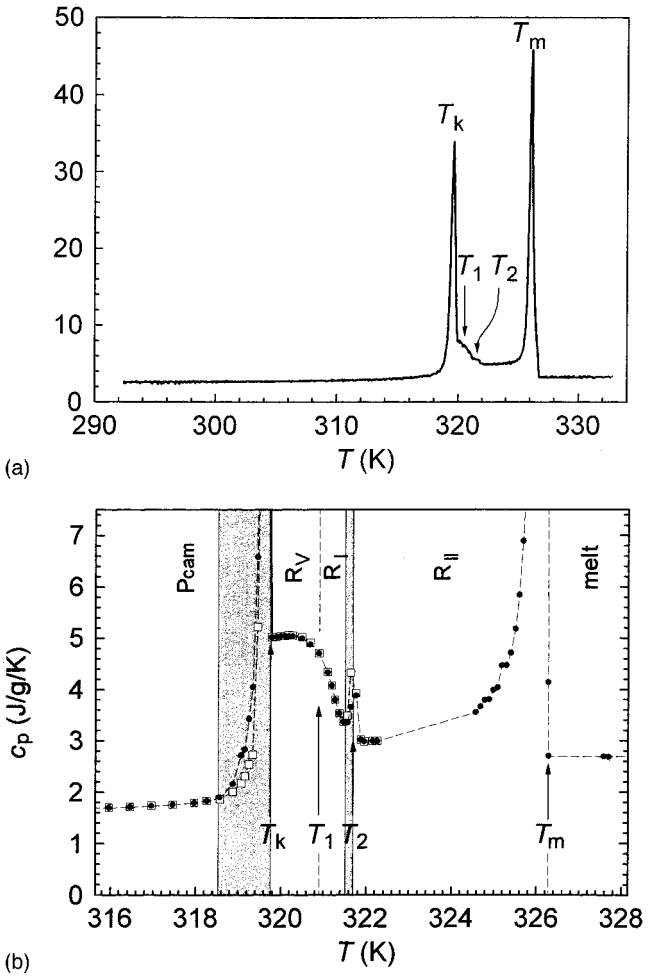

FIG. 2. (a) Temperature dependence of the specific heat c_p of $C_{25}H_{52}$ as obtained by the usual MDSC technique. (b) Quasi-isothermal c_p curve for different temperatures applying the time-domain-MDSC method. The dots represent the instantaneous response of c_p (c_p^i) after a positive temperature jump. The open squares give the relaxed values of c_p (c_p^r). R_V, R_I, and R_{II} represent the different rotator phases (Ref. 30).

The accuracy of the transition temperatures as revealed from BS depends on (i) the accuracy of the temperature determination itself (± 0.1 K), (ii) the temperature lag between the position of the temperature sensor and the scattering volume ($V_{\text{scattering}} \approx 10^{-8}$ cm^3), (iii) the temperature inhomogeneity within the sample due to the large heat capacity and the small thermal conductivity, (iv) the accuracy of the determination of the Brillouin frequencies ($\Delta f/f \approx 0.005$), and (v) the identification of the acoustic anomalies accompanying the phase transitions (± 0.3 K). Because of these manifold sources of experimental errors the absolute temperature accuracy of the transition temperatures as revealed by our Brillouin measurements is believed to be ± 0.6 K.

III. RESULTS AND DISCUSSION

Figure 2(a) shows an overview over our MDSC measurement on raw $C_{25}H_{52}$ performed with a heating rate of 0.06 K/min. The general shape of our calorimetric results is in accordance with those of Sirota *et al.* measured with an al-

TABLE I. Characteristic temperatures of $C_{25}H_{52}$ obtained by different experimental techniques. MDSC (modulated differential scanning calorimetry), BS (Brillouin spectroscopy). The two temperatures of Ref. 9 correspond to a heating and a cooling run. For more information see text.

	Reference	T_k (K) $Pcam \rightarrow R_V$	T_1 (K) $R_V \rightarrow R_I$	T_2 (K) $R_I \rightarrow R_{II}$	T_m (K) $R_{II} \rightarrow$ Melt
X-ray	28	320.6		324.1	$\geqslant$327
X-ray	29	320.8		322.4	326.7
X-ray	30	318.45	320.85	322.05	326.3
Calorimetry	9	320.1/319.1	321.45	322.1	327.05
MDSC		319.7	321	321.8	326.2
BS		320	322	324.1	327

ternative calorimetric technique.[9] The estimated transition temperatures are given in Table I and agree roughly with data given in the literature.[9,28–30] It is worth noting, that the transitions at T_1 and T_2 only show weak c_p anomalies and therefore demand a better resolving measurement technique (see below).

In Fig. 3 we give an overview over our Brillouin investigations on single-crystalline films of $C_{25}H_{52}$ on the PIA substrate. Both MDSC and BS give the same transition temperatures T_k and T_m (see Table I). From these coincidences, together with the fact that the PIA-prepared samples show at ambient temperature the lattice parameters a, b, and c of the natural phase,[32] we conclude that our PIA-prepared samples are representative for ordinary crystals as grown from solution or from the melt. However, the melting temperatures T_m as determined by MDSC and BS deviate by 0.8 K which is at the upper bound of the margin of error of both methods (see below).

Obviously, there exists a strong coupling between the driving order parameters at the transitions at T_k and T_m leading to significant discontinuities of the longitudinal elastic stiffness coefficients c_{22} and c_{33} and the shear stiffness c_{44}. Of course, these discontinuities are not just due to the related density anomalies but reflect strong morphologic influences. In this context it is interesting to compare the values of the elastic constants obtained by the Brillouin spectroscopy with the values of the linear isothermal compressibilities obtained by Sirota *et al.*[30] In the crystalline orthorhombic phase we can compare the elastic compliance s_{33} with the isothermal compressibility along the crystallographic c axis

$$\left(-\frac{1}{d}\frac{\delta d}{\delta P}\right) s_{33} = 2.9\times 10^{-11}\ \text{GPa};$$

$$-\frac{1}{d}\frac{\delta d}{\delta P} = 3.57\times 10^{-11}\ \text{GPa}.$$

Taking into account the very different frequency regime of both experimental methods, it is interesting to note the similarity of the obtained values. In the rotator phase R_{II} the isothermal compressibility increases to 6.74×10^{-11} GPa. We observe a clear decrease in c_{33} but unfortunately we cannot give an accurate value of s_{33} because we should count with the complete elastic tensor in order to calculate the real values of the compliances ($s_{33} \neq 1/c_{33}$).

Transition from $Pcam \rightarrow R_V$: A better resolved representation of $c_{22}(T)$ and $c_{33}(T)$ is given in Figs. 4 and 5. At T_k a dramatic jump of c_{33} (longitudinal elastic modulus parallel to the crystallographic c axis) by a factor of 9 is observed (Fig. 4). This observation is in line with the x-ray observation[30] that at T_k a sudden inclination of the preferential molecular axis of about 10° with respect to the c axis of the room-temperature phase takes place. At the same temperature the hypersonic attenuation Γ_{33} increases significantly (Fig. 4) supporting the idea of a translation-rotation coupling be-

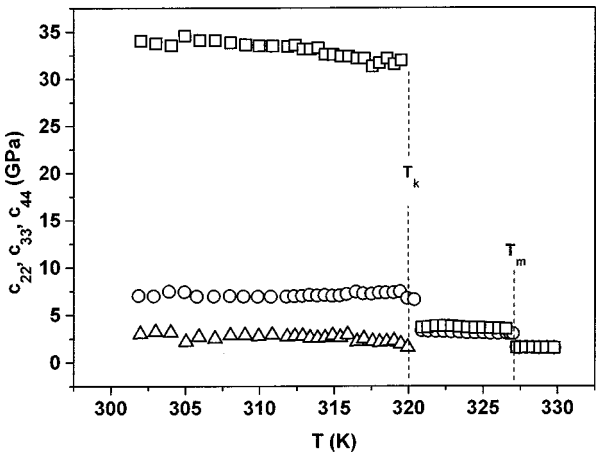

FIG. 3. Temperature dependence of the elastic constants $c_{22}(\bigcirc)$, $c_{33}(\square)$, and $c_{44}(\triangle)$. The density values used to calculate the elastic constants are given in the text.

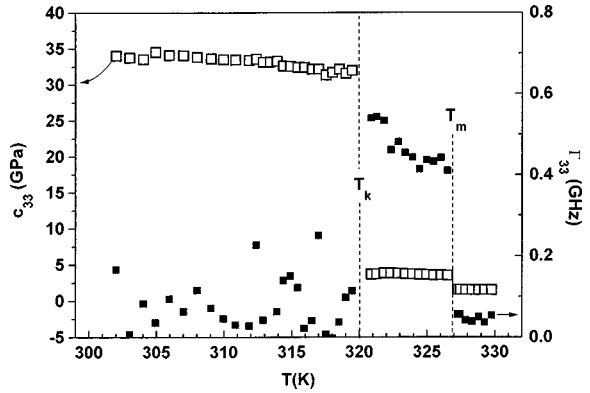

FIG. 4. Temperature dependence of the elastic constant c_{33} and the corresponding hypersonic attenuation Γ_{33} between $T=300$ and 330 K. The values of the transition temperatures T_k and T_m are given in Table I.

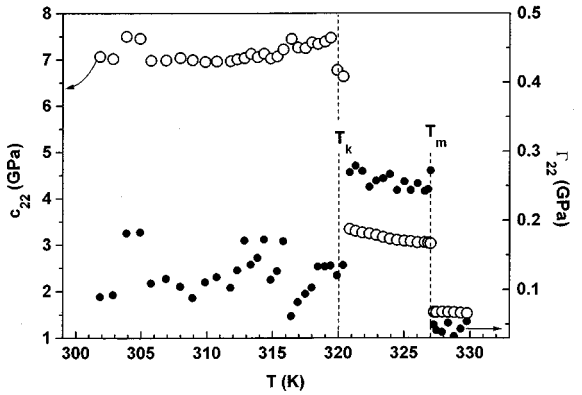

FIG. 5. Temperature dependence of the elastic constant c_{22} and the corresponding hypersonic attenuation Γ_{22} between $T=300$ and 330 K. The values of the transition temperatures T_k and T_m are given in Table I.

tween the longitudinal strain S_3 and the molecular tilting angle, one of the order parameters of this transition.

From Fig. 5 it is evident that the order parameter for the transition at T_k also couples to the elastic strain S_2 (Voigt's notation). As a matter of fact, on passing T_k from below, $c_{22}(T)$ significantly jumps from about 7 to about 3.35 GPa. Keeping in mind that the molecular tilting takes place in the crystallographic (a,c) plane,[30] it is unlikely that the jump of c_{22} is directly related to the lattice distortion. Since the transition from the room-temperature phase into the phase R_V is accompanied by a lattice expansion of 8% although the crystallographic b axis (=two axis of the sample) decreases by 1%, the strong decrease of c_{22} by more than a factor of 2 must be related to the lattice dynamics. Indeed, the molecular tilting at T_k is accompanied by the onset of molecular ''rotations'' along the molecular axis.[30] This additional degree of freedom has been attributed to the appearance of kink defects (see Refs. 3 and 4). The decrease of c_{22} and the related increase of Γ_{22} is likely due to a coupling between the elastic deformation S_2 and this dynamic intramolecular disordering of the $C_{25}H_{52}$ molecules. This order-disorder effect destroys the all-trans conformation of the chain molecules. The value and the temperature dependence of $\Gamma_{22}=(q^2/4\pi\rho)\eta_{22}$ suggests the appearance of a rather high structural viscosity[41] η_{22} within the rotator phases when compared with the values in the orthorhombic crystalline phase, being almost independent of temperature. As a matter of fact, the η_{22} values in the rotator phase are also higher than those of other plastic crystals in their rotator phases. In the case of symmetrical difluortetrachlorethane[42] the structural viscosity in the rotator phase is $\eta_{22}=8.2\times10^{-2}$ P, while in $C_{25}H_{52}$ it is $\eta_{22}=9.2\times10^{-2}$ P. This result indicates that the concentration of the dynamical intramolecular defects, relevant for the rather strong attenuation Γ_{22}, at Brillouin frequencies (GHz regime), remains almost constant until the melt transition.

The rather complicated behavior of the microscopical mechanisms, which drive the first-order transition at T_k, also emerges from our TDMDSC measurements. The TDMDSC technique allows the study of slow dynamical thermal effects which become relevant in the vicinity of phase transitions. Figures 2(b) and 6(a) demonstrate that there exist c_p relaxations in a temperature interval $[T_k-1.2\ \mathrm{K},\ T_k]$. In Fig. 6(a)

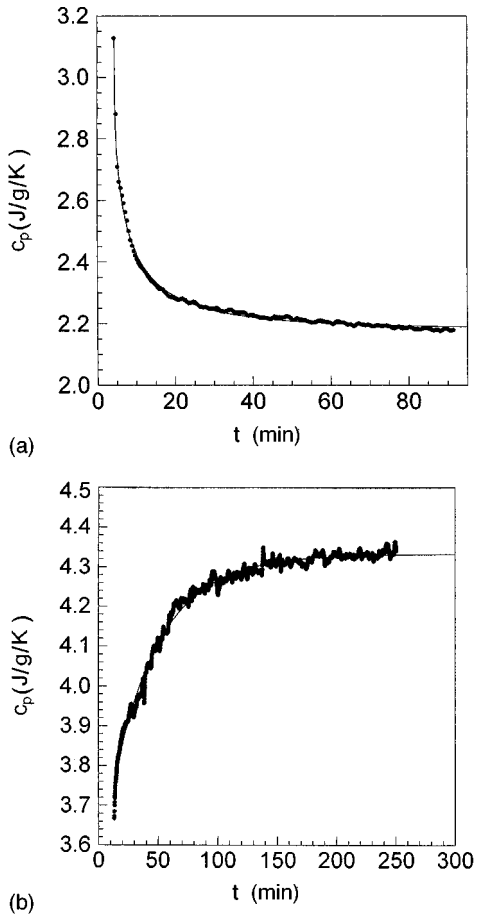

FIG. 6. Time dependence of c_p at (a) $T=319.1$ K and (b) $T=321.6$ K after a temperature step of 0.1 K. The relaxation curves were fitted according to a Kohlrausch-Williams-Watts law (Ref. 40).

a typical c_p versus time relaxation curve is shown at the average sample temperature $\langle T\rangle=319.1$ K. Interestingly, when performing a positive temperature step, the instantaneous c_p response after temperature stabilization, c_p^i, exceeds the relaxed response c_p^r below T_k [see Fig. 2(b)]. We attribute the increase of both the instantaneous and the relaxed specific-heat capacity, as before, to the onset of the dynamical intramolecular disorder on approaching T_k. However, whereas BS probes molecular motions within the microwave regime, TDMDSC probes only the accompanying slow structural relaxations due to defect redistributions. The temporal responses $c_p(t)$ could not be fitted by a simple exponential indicating that this relaxation process cannot be caused by a single dynamical process. In order to take into account the stretched-exponential curvature of our $c_p(t)$ data, we used tentatively as a fit function a Kohlrausch-Williams-Watts function.[40] This procedure yielded the average relaxation time $\langle\tau_{Tk}\rangle$ given in Fig. 7 (□). As a matter of fact, $\langle\tau_{Tk}\rangle$ strongly increases with increasing temperature and shows a tendency to diverge at T_k.

The relaxation process itself can be understood as follows: in a small temperature range of about 1.2 K below T_k a small positive temperature step $+\Delta T$ spontaneously increases the concentration of the intramolecular kink defects. Immediately after their creation the additional intramolecular

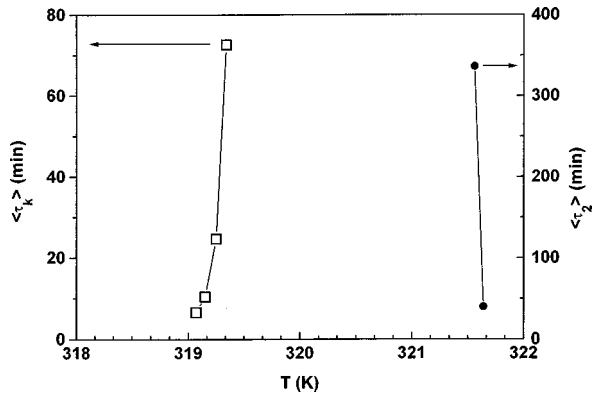

FIG. 7. Temperature dependence of the mean relaxation times $\langle \tau_I \rangle$ and $\langle \tau_2 \rangle$ around T_k and T_2 (see Table I).

defects are distributed rather randomly, destabilizing the orthorhombic phase. With increasing time, these defects are redistributed in the sense that the orthorhombic phase is stabilized. As can been seen in Fig. 7, close to T_k this average redistribution time $\langle \tau_{Tk} \rangle$ of the intramolecular defects becomes larger than 1 h. At a critical defect concentration, the average molecular all-trans conformation is definitely destroyed, the crystal lattice becomes unstable, and transforms into the tilted state.

Transition from R_V to R_I: The transition from the R_V phase into the R_I phase [Fig. 2(b)] manifests itself by a strong bending of the $c_p(T)$ curve around T_1, reflecting the second-order character of this transition. Within the phase R_I the $c_p(T)$ curve shows a plateau with a steep descent around $T_1 \approx 321$ K. According to Ref. 30, the tilt angle decreases on approaching T_1 from 10° to 5° before reducing to zero at T_1. Astonishingly, this reduction of the tilt angle is reflected by the related sensitive stiffness modul (Fig. 8) only through a slight increase of c_{33} and a small drop of the hypersonic attenuation constant Γ_{33} anomaly at $T_1 = 322$ K.

The increase of $c_{33}(T)$ until $T_1 = 322$ K (Fig. 8) is very similar to that found in other systems showing rotation-translation coupling[42] and is due to the coupling between the relevant strain component and the order parameter. The maximum of c_{33} at T_1 is not accompanied by a similar behavior of c_{22} (Fig. 9). This fact indicates the selectivity of the elastic strain tensor in relation to the ordering process.

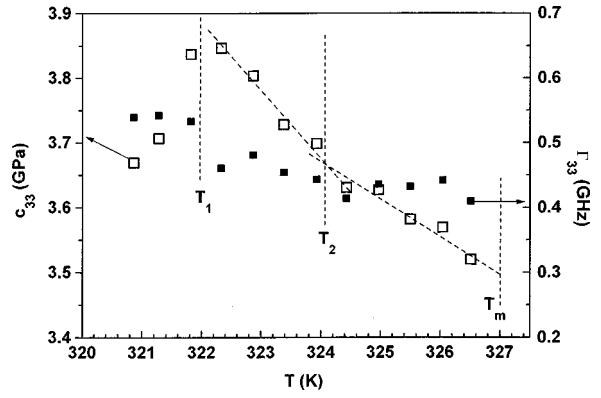

FIG. 8. Temperature dependence of the elastic constant c_{33} and the corresponding hypersonic attenuation Γ_{33} between $T = 320$ and 327 K. The dashed lines guides to the eye. The values of the transition temperatures T_1 and T_2 are given in Table I.

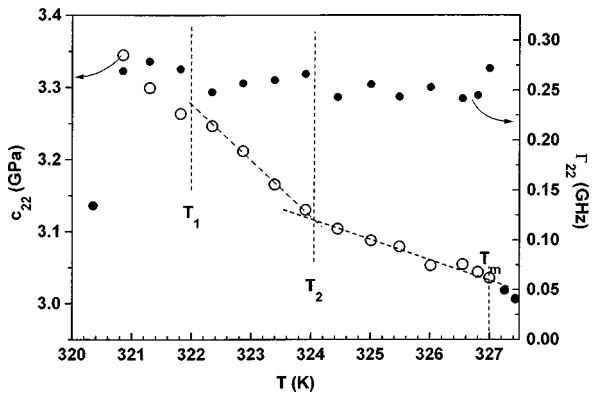

FIG. 9. Temperature dependence of the elastic constants c_{22} and the corresponding hypersonic attenuation Γ_{22} between $T = 320$ and 327 K are guides to the eye. The values of the transition temperatures T_1 and T_2 are given in Table I.

With respect to the expected translation-rotation coupling, $c_{44}(T)$ and $c_{55}(T)$ should be sensitive to the molecular tilting.[42] We were able to measure $c_{44}(T)$ below T_k (Fig. 3), but unfortunately we could not detect any of the shear stiffness moduli above T_k. Since we were even not able to detect the quasitransverse mode polarized in the (2,3) plane, e.g., at $\Phi = 45°$, we conclude that at least the shear stiffness c_{44} must be extremely weak. However for stability reasons of the crystal c_{44} cannot be zero. It can be very close to zero as has been shown in Refs. 6–8 and 25. As a result of our previous investigations on *n*-alkanes and perfluoralkanes, [6–8] we estimate an upper limit for the shear constant c_{44} in the rotator phase of alkanes: $c_{44} = 0.05$ GPa.

Transition from $R_I \rightarrow R_{II}$: In accordance with the results of Sirota *et al.*, we find in our calorimetric measurements a first-order transition at $T_2 \approx 321.8$ K. As a matter of fact, a further slow c_p-relaxation process is observed just below this weak first-order transition [Figs. 2(b), 6(b)] with average relaxation times $\langle \tau_{T2} \rangle$. This relaxation process is less pronounced compared to that at T_k [Figs. 6(a), 7]. In contrast to the relaxation process observed at T_k [Fig. 6(a)] the relaxed c_p^r at T_2 [Fig. 6(b)] exceeds that of the instantaneous value c_p^i and the relaxation time decreases on approaching T_2 (Fig. 7).

Tentatively we ascribe this calorimetric relaxation to the creation of a kind of defect, not relevant for the dynamical elastic properties at Brillouin frequencies (Γ remains constant). This kind of defect could be the well-known longitudinal diffusion motion of the molecular chains.

Such a mechanism has been already discussed for $C_{33}H_{68}$, $C_{20}F_{42}$, and $C_{24}F_{50}$.[3,6,8] From the fact that the relaxed c_p^r exceeds the instantaneous value c_p^i and from the large relaxation time, we conclude that close to the phase transition the equilibrium disorder exceeds the instantaneous one and that it takes macroscopic times to saturate the disorder of the system. Although the transition from phase R_I to R_{II} is of first order, this relaxation behavior indicates a continuous onset of structural disorder within the R_I phase prior to the phase transition at T_2.

An eventual effect of impurities on the c_p relaxation behavior probably can be excluded for at least two reasons: (i) The relaxation tendency is different at T_k and T_2 and (ii) no such relaxation was observed prior to the final melting transition.

Although the first-order structural transition at $T_2 \approx 322$ K is clearly seen in the calorimetric results, the elastic moduli c_{22} and c_{33} for $T_k < T < 322$ K give no hints for any further acoustic discontinuity (Figs. 8, 9) prior to the melting temperature T_m. However, both $c_{22}(T)$ and $c_{33}(T)$ show a kinklike behavior at about $T = 324$ K. This temperature deviates about $+2$ K from T_2 which exceeds the margin of experimental error. This holds especially true if we take into account that the maximum deviation between the other transition temperatures remain within less than 1 K and that the transition temperatures were determined in one BS measurement run using always the same temperature sensor. If we, nevertheless, attribute the temperature at the kink to the transition temperature T_2, we have to admit that the interaction field applied by the PIA substrate to the sample slightly shifts T_2 (and eventually T_m) to higher temperatures. Such a field effect is well known in the case of magnetic and ferroelectric phase transitions.

IV. SUMMARY

Taking advantage of the PIA-growth technique, large single crystals of $C_{25}H_{52}$ could be prepared which enabled us to investigate the dynamic and static elastic behavior around the various structural phase transitions of this material by Brillouin spectroscopy. In the crystalline orthorhombic phase typical values of the elastic constants are: $c_{22} = 7$ GPa, $c_{33} = 32$ GPa, $c_{44} = 2$ GPa. In the R_V orthorhombic rotator phase typical values of the elastic constants are: $c_{22} = 3.35$ GPa, $c_{33} = 3.67$ GPa, $c_{44} < 0.05$ GPa.

Calorimetric investigations within the time domain give some further insight into the static and dynamic thermal properties of the material. Moreover, it seems that the PIA substrate in some cases acts as a non-neglectable order-parameter field which may shift the phase-transition temperatures.

ACKNOWLEDGMENT

This work was kindly supported by the Deutsche Forschungsgemeinschaft.

*Present address: Instituto de Ciencia de Materiales de Madrid (CSIC) Cantoblanco, E-28049-Madrid, Spain.

[1] T. Albrecht, R. Jaeger, W. Petry, R. Steiner, G. Strobl, and B. Stühn, J. Chem. Phys. **95**, 2817 (1991).
[2] T. Albrecht, H. Elben, R. Jaeger, M. Kimmig, R. Steiner, G. Strobl, B. Stühn, H. Schwickert, and C. Ritter, J. Chem. Phys. **95**, 2807 (1991).
[3] G. R. Strobl, Colloid Polym. Sci. **256**, 427 (1978).
[4] G. Strobl, B. Ewen, E. W. Fischer, and W. Piesczek, J. Chem. Phys. **61**, 5257 (1974); W. Piesczek, G. R. Strobl, and K. Malzahn, Acta Crystallogr. Sect. B **30**, 1278 (1974).
[5] M. Möller, H.-J. Cantow, J. K. Krüger, and H. Höcker, Polym. Bull. **5**, 125 ff (1981).
[6] A. Marx, J. K. Krüger, and H.-G. Unruh, Z. Phys. B **75**, 101 (1989).
[7] R. Jiménez, J. K. Krüger, M. Prechtl, C. Grammes, and P. Alnot, J. Phys.: Condens. Matter **6**, 10 977 (1994).
[8] R. Jiménez, J. K. Krüger, C. Fischer, K.-P. Bohn, V. Dvorák, J. Holakovský, and P. Alnot, Phys. Rev. B **51**, 3353 (1995).
[9] E. B. Sirota and D. M. Singer, J. Chem. Phys. **101**, 10 873 (1994).
[10] J. K. Krüger, H. Bastian, G. I. Asbach, and M. Pietralla, Polym. Bull. **3**, 633 (1980).
[11] J. K. Krüger, M. Pietralla, and H.-G. Unruh, Phys. Status Solidi A **71**, 493 (1982).
[12] R. Boistelle, in *Current topics in Material Science*, edited by E. Kaldis (North-Holland, Amsterdam, 1980), Vol. 4.
[13] W. Pechhold, W. Dollhopf, and A. Engel, Acustica **17**, 61 (1966).
[14] D. Heyer, U. Buchenau, and M. Stamm, J. Polym. Sci. **22**, 1515 (1984).
[15] U. Buchenau, Solid State Commun. **32**, 1329 (1979).
[16] G. R. Strobl and R. Eckel, J. Polym. Sci. **14**, 913 (1976).
[17] G. R. Strobl, Colloid Polym. Sci. **254**, 170 (1976).
[18] R. G. Snyder, H. L. Strauss, R. Alamo, and L. Mandelkern, J. Chem. Phys. **100**, 5422 (1994).
[19] A. Marx, J. K. Krüger, and H.-G. Unruh, Appl. Phys. A **47**, 367 (1988).
[20] A. Marx, J. K. Krüger, A. Kirfel, and H.-G. Unruh, Phys. Rev. B **42**, 6642 (1990).
[21] J. C. Wittmann and P. Smith, Nature (London) **352**, 414 (1991).
[22] J. K. Krüger, M. Prechtl, P. Smith, S. Meyer, and J. C. Wittmann, J. Polym. Sci. B **30**, 1173 (1992).
[23] J. K. Krüger, M. Prechtl, J. C. Wittmann, S. Meyer, J. F. Legrand, and G. D'Asseza, J. Polym. Sci. B **31**, 505 (1993).
[24] C. Grammes, J. K. Krüger, K.-P. Bohn, J. Baller, C. Fischer, C. Schorr, D. Rogez, and P. Alnot, Phys. Rev. E **51**, 430 (1995).
[25] J. K. Krüger, C. Grammes, R. Jiménez, J. Schreiber, K.-P. Bohn, J. Baller, C. Fischer, D. Rogez, C. Schorr, and P. Alnot, Phys. Rev. E **51**, 2115 (1995).
[26] D. Fenwick, P. Smith, and J. C. Wittmann, J. Mater. Sci. **31**, 128ff (1996).
[27] M. G. Broadhurst, J. Res. Natl. Bur. Stand. Sect. A **66**, 241 (1962).
[28] J. Doucet, I. Denicolò, and A. F. Craievich, J. Chem. Phys. **75**, 1523 (1981); **75**, 5125 (1981); **78**, 1465 (1983).
[29] G. Ungar, J. Chem. Phys. **87**, 689 (1983).
[30] E. B. Sirota, H. E. King, D. M. Singer, and H. Shao, J. Chem. Phys. **98**, 5809 (1993).
[31] R. Jiménez, J. K. Krüger, K.-P. Bohn, and C. Fischer, J. Phys.: Condens. Matter **8**, 7579 (1996).
[32] B. Servet (private communication).
[33] K.-P. Bohn, A. Prahm, J. Petersson, and J. K. Krüger, Thermochim. Acta (to be published).
[34] M. Reading, B. K. Hahn, and B. S. Crowe, U.S. Patent No. 5,224,775 (6 July 1993); A. Boller, Y. Jin, and B. Wunderlich, J. Therm. Anal. **42**, 307 (1994).
[35] J. K. Krüger, L. Peetz, and M. Pietralla, Polymer **19**, 1397 (1978).
[36] J. K. Krüger, M. Pietralla, and H.-G. Unruh, Colloid Polym. Sci. **261**, 409 (1983).
[37] J. K. Krüger, A. Marx, L. Peetz, R. Roberts, and H.-G. Unruh, Colloid Polym. Sci. **264**, 403 (1986).
[38] J. K. Krüger, in *Optical Techniques to Characterize Polymer Systems*, edited by H. Bässler (Elsevier, Amsterdam, 1989).

[39] B. A. Auld, *Acoustic fields and waves in solids* (Wiley, New York, 1973).
[40] W. Williams and D. C. Watts, Trans. Faraday Soc. **66**, 80 ff (1970).
[41] L. D. Landau and E. M. Lifschitz, *Lehrbuch der Theoretischen Physik VII* (Akademie-Verlag, Berlin, 1975).
[42] J. K. Krüger, J. Schreiber, R. Jiménez, K.-P. Bohn, F. Smutný, M. Kubatt, J. Petzelt, J. Hrabovská-Bradshaw, S. Kamba, and J. F. Legrand, J. Phys.: Condens. Matter **6**, 6947 (1994).